

# Illicit Transport via Dipeptide Transporter Dpp is Irrelevant to the Efficacy of Negamycin in Mouse Thigh Models of *Escherichia coli* Infection

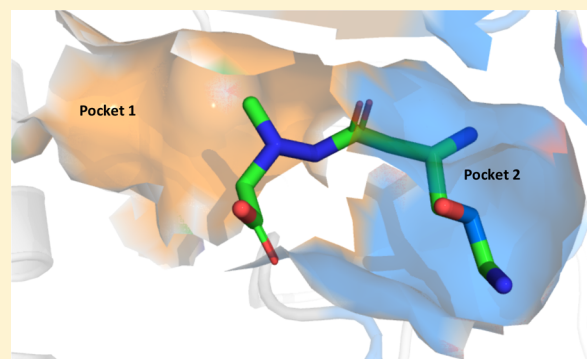
David C. McKinney,<sup>†</sup> Natascha Bezdenezhnik-Snyder,<sup>†</sup> Krista Farrington,<sup>‡</sup> Jian Guo,<sup>§</sup> Robert E. McLaughlin,<sup>‡</sup> Anatoly M. Ruvinsky,<sup>†</sup> Renu Singh,<sup>‡</sup> Gregory S. Basarab,<sup>†</sup> Sridhar Narayan,<sup>†</sup> and Ed T. Buurman<sup>\*,‡</sup>

<sup>†</sup>Departments of Chemistry, <sup>‡</sup>Biosciences, and <sup>§</sup>Drug Metabolism and Pharmacokinetics, Infection Innovative Medicines Unit, AstraZeneca R&D Boston, 35 Gatehouse Drive, Waltham, Massachusetts 02451, United States

## Supporting Information

**ABSTRACT:** Negamycin is a hydrophilic antimicrobial translation inhibitor that crosses the lipophilic inner membrane of *Escherichia coli* via at least two transport routes to reach its intracellular target. In a minimal salts medium, negamycin's peptidic nature allows illicit entry via a high-affinity route by hijacking the Dpp dipeptide transporter. Transport via a second, low-affinity route is energetically driven by the membrane potential, seemingly without the direct involvement of a transport protein. In mouse thigh models of *E. coli* infection, no evidence for Dpp-mediated transport of negamycin was found. The implication is that for the design of new negamycin-based analogs, the physicochemical properties required for cell entry via the low-affinity route need to be retained to achieve clinical success in the treatment of infectious diseases. Furthermore, clinical resistance to such analogs due to mutations affecting their ribosomal target or transport is expected to be rare and similar to that of aminoglycosides.

**KEYWORDS:** aminoglycosides, ribosome, negamycin, dipeptide, efficacy, membrane potential



Illicit transport is the term coined for the cellular entry of antibacterial compounds via transporters that are designed for other, physiological substrates.<sup>1</sup> This phenomenon has been observed for a wide range of transporters and chemical compound classes, including many natural products. D- $\alpha$ -Hydrazinoimidazolepropionic acid and azaserine, homologues of histidine and glutamine, hijack amino acid permeases hisP and aroP, respectively, to reach their respective intracellular targets.<sup>2</sup> The transport of albomycin via siderophore uptake systems and subsequent hydrolysis of its ferrichrome moiety is required to release its antibacterial component, a seryl tRNA synthetase inhibitor.<sup>3,4</sup> Fosfomycin and fosmidomycin both utilize hexosephosphate transporter Uhp and glycerol-3-phosphate carrier GlpT to gain access to the cytosol where they inhibit their targets, UDP-GlcNAc-enolpyruvyl transferase and 1-deoxy-D-xylulose-5-phosphate reductoisomerase, respectively.<sup>5–8</sup> Illicit transport seems to be one of the solutions exploited by microbial producers to deliver antibiotics too large and/or too polar for passive diffusion across the bacterial membrane(s) into the cytosol of surrounding species and thus gain a competitive advantage.

Negamycin ([2-[(3R,5R)-3,6-diamino-5-hydroxyhexanoyl]-1-methylhydrazino] acetic acid) is an antibacterial dipeptide-like natural product linking  $\delta$ -hydroxy- $\beta$ -lysine and methylhydrazino-

noacetic acid via a peptide bond (Table 1).<sup>9</sup> Isolated 45 years ago from fermentation broths of *Streptomyces purpeofuscus*, it is a bactericidal translation inhibitor with demonstrated efficacy in immunocompetent murine sepsis models.<sup>10,11</sup> Its broad antibacterial spectrum includes *Pseudomonas aeruginosa*, *Acinetobacter baumannii*, and *Enterobacteriaceae*, pathogens for which medical treatment options are dwindling rapidly because of the emergence of clinical resistance to existing drug classes.<sup>12</sup> Recently, X-ray crystal structures showed negamycin to bind in a location overlapping with that of tetracycline in the 30S subunit of 70S ribosomes obtained from *Escherichia coli* and *Thermus thermophilus*.<sup>13,14</sup> Single-molecule fluorescence resonance energy transfer measurements mechanistically demonstrated the stabilization of near-cognate tRNA binding in the A site upon binding of negamycin followed by misincorporation, molecular events not observed with either tetracycline or tigecycline.<sup>13,15</sup> Therefore, these findings provide a structural foundation for the rational design of biochemically more potent, bactericidal negamycin analogs.

Negamycin is a multiprotic compound with very low lipophilicity ( $\log D_{7.4} < -1$ ), which therefore makes it unlikely

Received: March 5, 2015

Published: March 31, 2015

Table 1. Biochemical and Antimicrobial Activity of Negamycin Stereoisomers<sup>a</sup>

Compound	Structure	TT	MHBII		M9+glucose	
			parent	$\Delta dppA$	parent	$\Delta dppA$
Negamycin (1) 3R5R		1.9	32	32	4	32
3-epi-Negamycin (2) 3S5R		16	512	512	8	64
5-epi-Negamycin (3) 3R5S		51	1024	1024	32	256
3,5-epi-Negamycin (4) 3S5S		8.7	512	512	4	128
gentamicin			1	1	1	1
tetracycline			1	1	0.5	0.5

<sup>a</sup>Biochemical activity was determined in a coupled transcription–translation assay (TT) using S30 extracts from *E. coli* MRE600 ( $IC_{50}$  in  $\mu M$ ,  $n > 2$ ) and their antimicrobial activity (MIC in  $\mu g/mL$ ,  $n = 3$ ) against *E. coli* ATCC25922 and its isogenic  $\Delta dppA$  derivative. The latter were determined in both a rich medium (cation-adjusted Mueller-Hinton broth (MHBII)) and a minimal salts medium (M9 + glucose).

to diffuse passively and rapidly through hydrophobic membranes, a notion supported by its low oral bioavailability in rats.<sup>16</sup> Raju et al. synthesized negamycin analogs with biochemical activity that failed to translate to commensurate antibacterial activity against *E. coli*, leading them to suggest the involvement of differential uptake mechanisms.<sup>17</sup> To complement the aforementioned structural tools for the design of better translation inhibitors with the rationale to maintain the access of negamycin in appreciable concentrations to the ribosome, its transport mechanisms into *E. coli* were determined. Here, two major routes of negamycin entry across the cytosolic membrane were demonstrated, a high-affinity mechanism by illicit transport via dipeptide transporter Dpp and a low-affinity route driven by the membrane potential. Under growth conditions prevalent in a standardized antibacterial susceptibility testing medium and infected mouse thigh tissue, illicit transport did not occur. Therefore, in the pursuit of negamycin analogs for clinical use as antibacterials, the design and synthesis of biochemically more potent inhibitors should be limited to those capable of exploiting the low-affinity mechanism of cell entry.

## RESULTS AND DISCUSSION

**Synthesis and Characterization of Negamycin Stereoisomers.** Negamycin was synthesized as previously described, resulting in a product with biochemical and microbiological activity indistinguishable from those of negamycin that was purified as a fermentation product (Table 1).<sup>13</sup> The compound was also biochemically equipotent to the literature precedent in coupled transcription–translation assays using S30 extracts prepared from *E. coli*, with inhibitory concentrations at which 50% of the activity remained ( $IC_{50}$ ) for 1 to 2  $\mu M$ .<sup>17</sup> Its antimicrobial activity against *E. coli*, as reflected by its minimum inhibitory concentration (MIC) of 32  $\mu g/mL$  in “rich” medium, using cation-adjusted Mueller–Hinton broth (MHBII) containing beef infusion and casein hydrolysate, was, however, 8-fold weaker than in previous reports (compare refs 13 and 14 with refs 10 and 17), whereas its activity against nonfermenters *Pseudomonas aeruginosa* and *Acinetobacter baumannii* was equivalent (Table S1).<sup>17</sup> Because negamycin contains two

chiral centers, the optimal stereochemistry for inhibitory potency was verified by synthesis and side-by-side characterization of the four possible stereoisomers (Table 1). The opposite enantiomer of negamycin with the 3S,5S configuration, compound 4, showed a 4- to 5-fold reduction in inhibitory biochemical potency and a 16-fold reduction in antibacterial activity in rich medium. Inversion of the individual chiral centers into 3S and 5S, compounds 2 and 3, reduced the biochemical potency 8- and 25-fold and the antimicrobial activity in rich medium 16- and 32-fold, thus showing that the 3R,5R configuration was optimal. Antimicrobial activity of negamycin against *E. coli* in a variety of rich media other than MHBII invariably reproduced its potency of an MIC of 32  $\mu g/mL$  (data not shown). However, when *E. coli* was grown in a defined minimal salts medium, M9 + glucose, an MIC value of 4  $\mu g/mL$  was obtained (Table 1), an 8-fold lowering. Moreover, the MIC values for the diastereomers of negamycin, compounds 2–4, in the minimal media decreased 64-, 32-, and 128-fold, respectively. The MIC values of neither gentamicin nor tetracycline were changed significantly in the minimal salts medium.

**Identification of a High-Affinity and a Low-Affinity Negamycin Transport Route.** To elucidate the mechanism that led to the improved activities for negamycin and its stereoisomers in the minimal salts medium, resistant mutants of *E. coli* W3110 were isolated at 4–8  $\mu g/mL$  negamycin, i.e., 1- to 2-fold its MIC. The resistance frequency was high,  $10^{-6}$ , and five randomly chosen colonies revealed upon whole-genome sequencing four different mutations that all involved the *dpp* operon which encodes the Dpp ATP-binding cassette transporter, including periplasmic binding protein DppA, transmembrane domains DppB and C, and nucleotide binding domains DppD and F.<sup>18</sup> The mutations found were an adenosine insertion in *dppA* resulting in a frame shift at I409, a deletion in DppC starting at R88, a D186Y point mutation in DppF (twice), and a 100 kb deletion that removed the entire *dppABCD* operon (Table S2). Under these conditions, no mutants were found that did not contain a mutation within the *dpp* operon.

Table 2. Antimicrobial Activity of Negamycin and Gentamicin against Deletion Strains from Keio Collection<sup>a</sup>

category	deletion	MHBII		M9 + glucose	
		negamycin	gentamicin	negamycin	gentamicin
control		16	1	2	0.5
Dpp operon	<i>dppA</i> , <i>dppB</i> , <i>dppC</i> , <i>dppD</i> , <i>dppF</i>	16–32	0.5–1	8–16	0.5
membrane potential	<i>ubiX</i>	>64	4	2	0.5
DppA homologues	<i>nika</i> , <i>oppA</i> , <i>sapA</i> , <i>mppA</i>	16–32	0.5–2	2–4	0.5–1

<sup>a</sup>Control is *E. coli* MG1655; “Dpp operon” and “membrane potential” strains contain deletions in loci linked to negamycin resistance in minimal salts medium M9 + glucose and rich medium MHBII, respectively.

Target-based resistant mutants of *E. coli* SQ110 containing a single rDNA copy have been previously isolated in rich medium at 128  $\mu\text{g/mL}$  negamycin, i.e., 4-fold the MIC, at a low frequency of  $10^{-9}$ .<sup>13,14</sup> At 32 and 64  $\mu\text{g/mL}$  negamycin in rich medium used here, however, the resistance frequencies were considerably higher,  $10^{-7}$ – $10^{-6}$ . Whole genome sequencing of eight isolates revealed mutations in *cpxA*,<sup>19</sup> *hem* genes,<sup>20</sup> and *ubi* genes,<sup>21</sup> which have all been linked to aminoglycoside resistance and/or components of the respiratory chain required to maintain the membrane potential (Table S2): a T91P point mutation (twice) and a deletion starting at A14 in UbiX, a nonsense mutation at Q183 in UbiF, a cytosine deletion resulting in a frame shift at E179 in UbiH, a G89S point mutation in HemB, a nonsense mutation at Q251 in HemL, and a A187 V point mutation in CpxA.

To confirm the phenotypes of spontaneous mutants isolated on minimal salts and rich medium, isogenic strains from the Keio collection were used that contain precise deletions of each of *dppA*–*ddpF*, of genes encoding periplasmic binding proteins with high homology to DppA, and of *ubiX*, a representative and most frequently isolated mutated gene shown to lead to a reduced membrane potential (Table 2). In the minimal salts medium, the deletion of any of the *dpp* genes increased the MIC from 2 to 4  $\mu\text{g/mL}$  to 8 to 16  $\mu\text{g/mL}$ , close to the 16 to 32  $\mu\text{g/mL}$  observed in rich medium. Because periplasmic binding proteins have the potential to interact with noncognate ATP-binding cassette transporters,<sup>22</sup> possible resistance of strains with deletions in genes encoding such proteins (*nika*, *oppA*, *sapA*, or *mppA*) was assessed but no elevation in MIC was observed (Table 2). In rich medium, the deletion of *dpp* genes did not increase the MIC of negamycin whereas the deletion of *ubiX* increased the MIC of negamycin at least 4-fold and that of gentamicin 2- to 8-fold.

Physiological evidence for the uptake of negamycin through Dpp was obtained by measuring the antimicrobial activity of negamycin in a minimal salts medium in the presence of L-Ala-L-Ala, a physiological substrate of the Dpp transporter.<sup>23,24</sup> Titration of the dipeptide revealed that 100  $\mu\text{M}$  increased the MIC of the wild-type strain from 4 to 32  $\mu\text{g/mL}$  whereas no effect of the addition was seen with the *dppA* mutant (Figure 1). Because the maximum MIC of 32  $\mu\text{g/mL}$  equals that observed for the wild type in rich medium, the enhanced uptake of negamycin in minimal medium seems exclusively due to uptake via Dpp. The membrane potential was varied by increasing the pH of MHBII medium from 5.5 to 9, leading to elevated membrane potentials.<sup>25</sup> The MICs of negamycin and gentamicin dropped 16- to 32-fold against both wild-type *E. coli* and *E. coli*  $\Delta dppA$  when raising the pH (Figure 2). A similar decrease was observed for *E. coli*  $\Delta ubiX$ , except that the curve was shifted to lower antimicrobial activity, in agreement with the reduced membrane potential due to the *ubiX* deletion.<sup>21</sup> In contrast, the antimicrobial activity of tetracycline against the

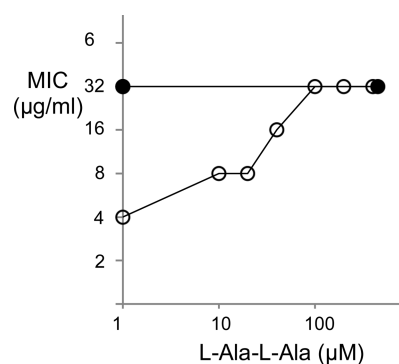


**Figure 1.** Antimicrobial activity of negamycin (MICs in  $\mu\text{g/mL}$ ;  $n = 3$ ) in M9 + glucose medium against *E. coli* ATCC25922 (open symbols) and its isogenic  $\Delta dppA$  derivative *E. coli* ARCS446 (closed symbols) in the presence of dipeptide L-Ala-L-Ala. Qualitatively similar results were obtained with compound 4 against this set of strains and for each compound against *E. coli* MG1655 and its  $\Delta dppA$  derivative (data not shown).

three strains was identical, all showing a 4-fold increase in MIC due to deprotonation of the phenolic  $\beta$ -ketone system, creating a charged species that would be less permeant above pH 7.7 relative to the neutral, permeant molecule below pH 7.7, thus reducing the intracellular antibiotic concentration.<sup>26,27</sup>

**Computational Analysis of Negamycin Binding to DppA.** Attempts were unsuccessful to obtain biophysical evidence for negamycin binding to DppA by setting up and reproducing published crystallographic systems of *E. coli* DppA (data not shown).<sup>28,29</sup> To explain why the DppA deletion plays a more profound role in increasing the MIC of the 3S,5S stereoisomer relative to that of the other diastereomers (Table 1) and to gain insight into the binding of the stereoisomers to *E. coli* DppA, an in silico model was developed using the published crystal structure of *E. coli* DppA in complex with dipeptide Gly-L-Leu (PDB ID 1dpp). The dipeptide binding site has two pockets: pocket 1 that binds the leucine side chain and pocket 2 that is near the  $C_{\alpha}$  atom of glycine, an open region oriented to accommodate any of the L-amino acids but much less so the D-amino acid side chains (Figure 3A).<sup>24,28</sup>

This preferred binding of L-amino acid-containing substrates is due to optimal orientation toward pockets 1 and 2.<sup>24,30</sup> The  $\pi$ -cation interaction enabled by the 3.4 Å proximity between the  $\pi$  system of W405 and the Gly-L-Leu terminal amino group corresponded to a 5.0 Å distance between the W405 indole six-membered ring and the 3R amino group of negamycin (Figure 4A). The 3R negamycin stereochemistry is equivalent to the replacement of the Gly of the dipeptide with D-amino acids that is known to weaken dipeptide binding to DppA.<sup>24</sup> Modeling also predicts stronger binding for 3S stereoisomers that can be attributed to the following three specific changes in the binding mode. First, the 3S configuration shifted the C3-amine closer to



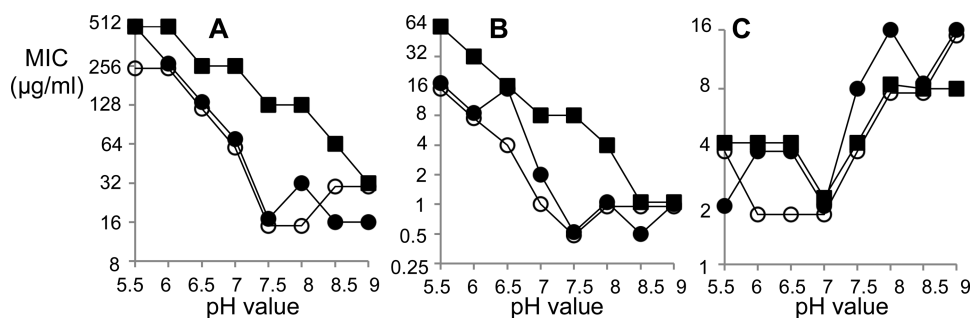


**Figure 2.** Antimicrobial activity (MICs in  $\mu\text{g}/\text{mL}$ ) of negamycin (A), gentamicin (B), and tetracycline (C) against *E. coli* MG1655 (open symbols) and its  $\Delta dppA$  (closed circles) and  $\Delta ubiX$  (closed squares) derivatives in MHBII medium buffered at different pH values. Similar results were obtained with *E. coli* ATCC25922 and its  $\Delta dppA$  derivative *E. coli* ARC5446 (data not shown).

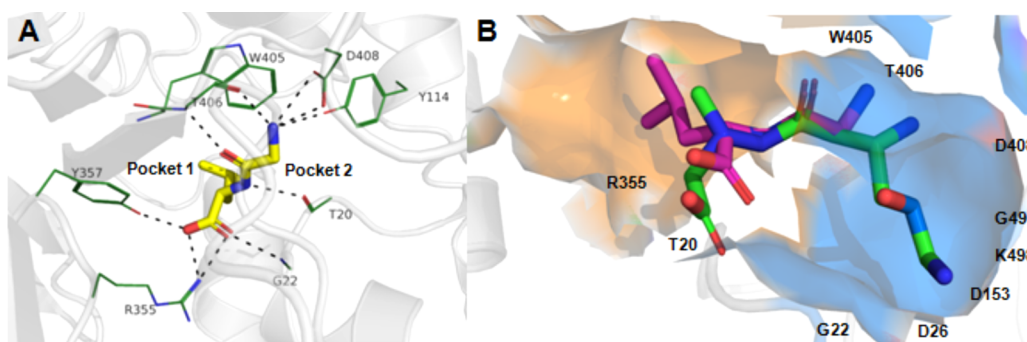


**Figure 3.** Crystal structure of Gly-L-Leu bound to *E. coli* DppA (PDB ID 1DPP) (A) and the model of negamycin binding to the protein (B). (A) Some of the key interactions between Gly-L-Leu (yellow) and the binding site residues (green) are shown by dashed lines. The Leu side chain extends into pocket 1. Carbon atoms are depicted in yellow, nitrogen atoms in blue, and oxygen atoms in red. (B) Surface representation of negamycin extending deep into pocket 2 (blue) but leaving pocket 1 (orange) virtually unoccupied. Carbon atoms are in pink (Gly-L-Leu) or in green (negamycin), nitrogen atoms are in blue, and oxygen atoms are in red.

the centroid of the W405 indole six-membered ring (cf. Figure 4BD,AC), resulting in 3.8 and 3.7 Å distances for the two 3S stereoisomers. Note that a complete disruption of the  $\pi$ -cation interaction by Trp to Ala substitution in *Pseudoalteromonas* sp. SM9913 DppA reduced dipeptide binding, illustrating the importance of the interaction.<sup>31</sup> Second, the 3R-to-3S inversion is predicted to strengthen the hydrogen bond interaction between the C3-amine and the hydroxyl group of Y114, decreasing the donor–acceptor distance from 3.8 to 2.9 Å. The third change relates to the negamycin’s 5-hydroxy-6-amine lysine moiety predicted to reach far into pocket 2, formed by G22, Y25, D153, P356, T406, G497, and K498 residues (Figure 3B). In all stereoisomers, the terminal C6-amine group interacts with the backbone carbonyl group of G497, but its engagement in two salt bridges with D26 and D408 mainly depends on the chirality of the C-3 atom. The 3S configuration allowed the interaction of the C6-amine with G497, D26, and D408 (Figure 4BD) and is therefore favorable over the 3R configuration, which allowed only one salt bridge with D26 in negamycin. Because the 3S,5S negamycin showed a 32-fold loss of antimicrobial activity in the minimal salts medium in the absence of DppA, instead of 8-fold observed for the other stereoisomers, the correct configuration of both chiral centers seems important (Table 1).

**Roles of Dpp in the Virulence of *E. coli* and Efficacy of Negamycin.** To evaluate the importance of Dpp in the establishment of *E. coli* infections and in particular its putative role in mediating the efficacy of negamycin, a  $\Delta dppA$  derivative of *E. coli* ATCC25922, *E. coli* ARC5446, was investigated in a neutropenic mouse thigh infection model. The bacterial thigh

burdens for wild-type *E. coli* ATCC25922 and its  $\Delta dppA$  derivative were  $7.0 \pm 0.4 \log_{10}$  CFU/g and  $6.6 \pm 0.2 \log_{10}$  CFU/g at  $t = 0$  h (Figure S4). After 12 h, the thigh burdens were  $9.0 \pm 0.3 \log_{10}$  CFU/g and  $8.8 \pm 0.3 \log_{10}$  CFU/g, respectively, suggesting that dipeptide uptake via this route has no impact on *E. coli*’s ability to proliferate and establish an infection. The administration of negamycin in the infection model against both *E. coli* ATCC25922 and its  $\Delta dppA$  derivative afforded a good dose response, providing further evidence of the minimal effect of Dpp-mediated transport (Figure 5). Only a modest reduction in efficacy was observed with *E. coli* ARC5446, increasing the total daily dose required for stasis from 75 to 150 mg/kg for the wild-type strain to 250 mg/kg for the  $\Delta dppA$  mutant (Figures 5 and 6), which is much smaller than the 8-fold increase in MIC that measurements in a minimal salts medium would predict (4 to 32  $\mu\text{g}/\text{mL}$ , Table 1). Furthermore, compound 2, which showed similar antimicrobial activity to negamycin in a minimal salts medium, was also administered against *E. coli* ATCC25922 in the model; however, no efficacy was observed up to the maximum tolerated dose of 800 mg/kg whereas an 8-fold-lower dose of negamycin was sufficient to result in stasis, despite its similar exposure to negamycin upon subcutaneous administration (Table S3).

In conjunction, the observations in the mouse model strongly suggest that negamycin does not gain entry into the cytosol via DppA into *E. coli* during infection and that antimicrobial activity determined in a rich medium is a more accurate reflection of its potency in vivo.

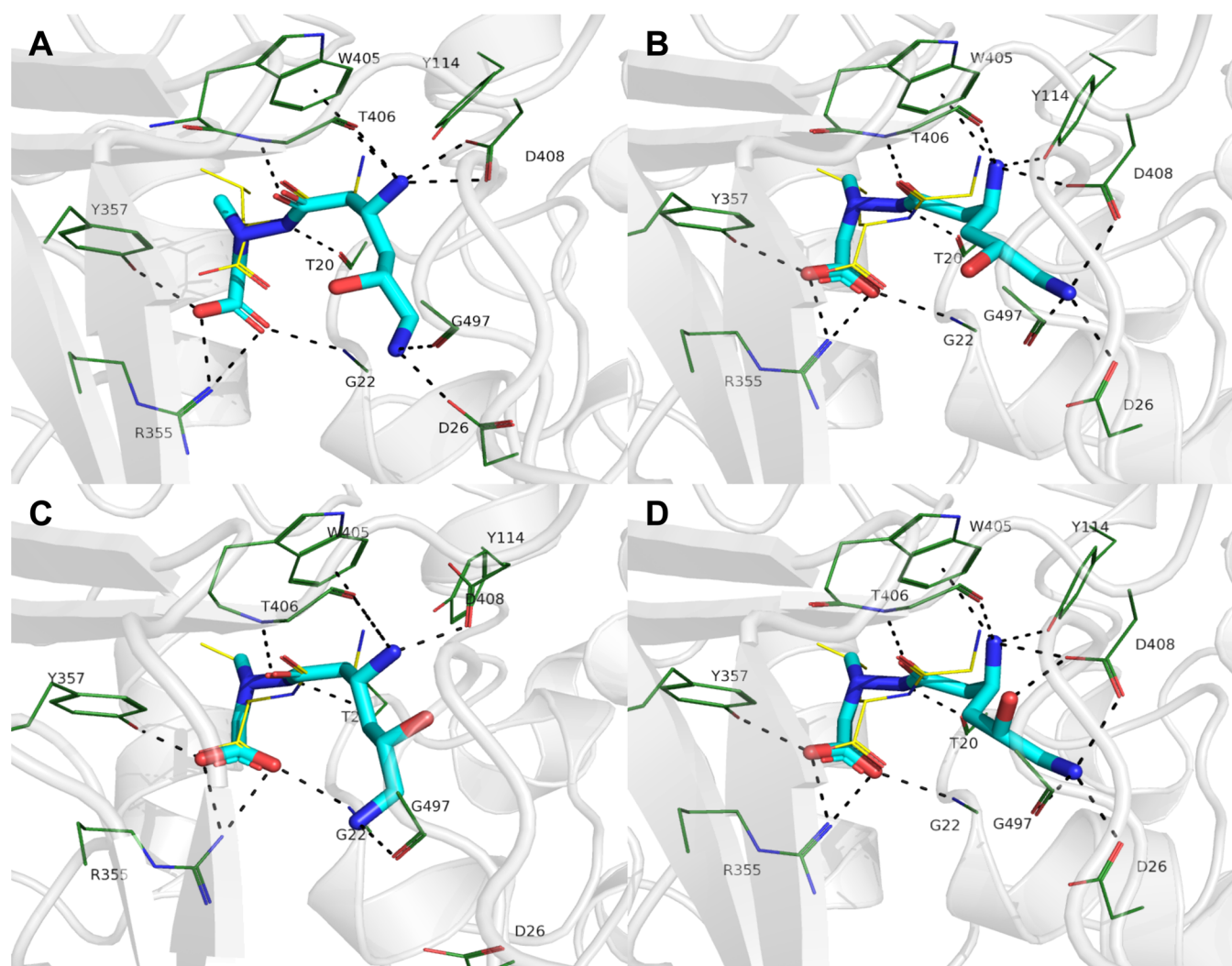


**Figure 4.** Predicted models of negamycin and its stereoisomers in the DppA binding site. Carbon atoms in the models are in cyan, whereas those in the Gly-L-Leu dipeptide are in yellow. Oxygen and nitrogen atoms are in red and blue, respectively. (A) Negamycin (3R,5R), (B) compound 2 (3S,5R), (C) compound 3 (3R,5S), and (D) compound 4 (3S,5S). Some of the key interactions are shown by dashed lines. Alignments of the models to the dipeptide were obtained by superposing corresponding structures of the binding site in PyMOL.<sup>52</sup>

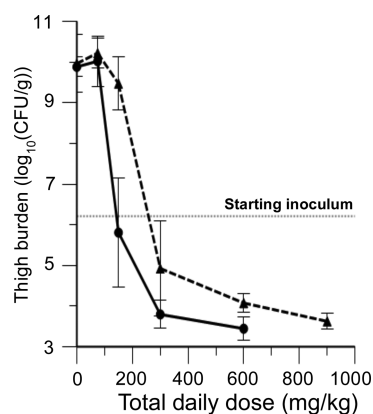


**Figure 5.** Efficacy of negamycin observed in immunocompromised mouse thigh models using *E. coli* ATCC25922 (circles) and its isogenic  $\Delta dppA$  derivative *E. coli* ARCS446 (triangles). The daily dose was administered in six equal fractions (q6). Thigh burdens (CFU/g, geometric mean  $\pm$  SE,  $n = 6$ ) were determined after 24 h.

**Concluding Remarks.** Negamycin is a very polar, dipeptide-like antimicrobial compound that has to cross both

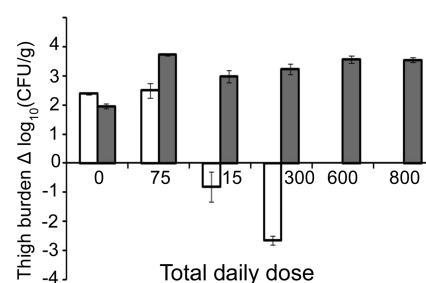


**Figure 6.** Change in bacterial thigh burden upon treatment with negamycin (light bars) and compound 2 (dark bars) against *E. coli* ATCC25922 in a neutropenic mouse model. The daily dose was administered in four equal fractions (q4). Thigh burdens (CFU/g, geometric mean  $\pm$  SE,  $n = 6$ ) were determined after 24 h. The pretreatment burden was  $(2.1 \pm 0.1) \times 10^6$  CFU/g.

the outer and inner membranes of Gram-negative pathogens such as *E. coli* in order to reach and bind its intracellular target, the 30S ribosomal subunit. Its mechanism of transport across the outer membrane has not been determined, but its single net positive charge at physiological pH and the small size of 250 D

support passive permeation through one or more of the hydrophilic porins.<sup>32,33</sup>

To gain entry to the cytosol across the hydrophobic inner membrane, the compound exploits at least two mechanisms, a high-affinity route by hijacking the Dpp transporter and a low-affinity route, driven by the membrane potential. In a minimal salts medium, i.e., in the absence of added dipeptides, antimicrobial activity with an MIC value of 4  $\mu\text{g}/\text{mL}$  was relatively high and resistance mutations that were isolated readily under these conditions all obliterated Dpp activity (Table S2). Dpp-mediated uptake of negamycin was also blocked by adding a physiological dipeptide substrate, L-Ala-L-Ala, to the minimal salts growth medium (Figure 1). Hence, the relatively low antimicrobial activity of negamycin in rich medium against wild-type *E. coli* is due to the combination of dipeptides in the medium outcompeting negamycin and the reduced expression of Dpp.<sup>34</sup>

It has been well established that the proton motive force is a composite of a chemical proton gradient and an electrical gradient across the cytoplasmic membrane of bacteria, including *E. coli*.<sup>35</sup> The universality of this mechanism combined with the conserved nature of the bacterial ribosome explains its broad antimicrobial spectrum against Gram-negative pathogens (Table S1). To maintain both this driving force for ATP synthesis and the cytoplasmic pH constant, the membrane potential, inside negative, is maximal around pH 7.5 and increasingly diminished, i.e., less negative, at lower pH values. Because negamycin with its  $\text{pK}_a$  values of 3.2, 8.0, and 9.6 carries a single positive charge at physiological pH,<sup>16</sup> it will be prone to entering the cell via the established electrical gradient. This hypothesis is supported by both the lower antimicrobial activity at low medium pH and decreased susceptibility due to mutations that lower the membrane potential (Table S2, Table 2, and Figure 2). Negamycin's physicochemical properties (charge and hydrophilicity) and its proposed membrane-potential-driven route of cell entry are therefore similar to those of aminoglycosides.<sup>25</sup>

Importantly, the search for negamycin-resistant mutants in a rich medium did not yield mutations in a membrane protein that would facilitate compound transfer and the rapid establishment of a distribution equilibrium dictated by the membrane potential, a result similar to those obtained with aminoglycosides.<sup>36</sup> The reliance of antibiotic entry on illicit transport via a single transporter creates a liability due to the relative ease with which highly resistant mutants with minimal fitness costs can be isolated.<sup>37</sup> Here, however, the illicit transport seen for negamycin in vitro did not appear to occur in vivo when negamycin transport seems to be mediated by the low-affinity route. Although mutants resistant to both negamycin and aminoglycosides were readily isolated in vitro, these are rare in the clinic even after decades of aminoglycoside usage, presumably because of the pleiotropic effect of the mutations in vivo.<sup>38</sup> Conceptually very similar, only a small subset of mecillinam-resistant mutants of *E. coli* with unaltered fitness was recently found to be clinically relevant.<sup>39</sup> By analogy to aminoglycosides, therefore, negamycin's molecular target and route of bacterial entry during infection predict a very slow development of clinical resistance of more potent analogs that retain these properties.

## METHODS

**Synthesis of Negamycin Stereoisomers.** Negamycin ([2-[(3*R*,5*R*)-3,6-diamino-5-hydroxyhexanoyl]-1-methylhydra-

zino] acetic acid) (1) and its 3*S*,5*R* stereoisomer (2) were synthesized as previously described (Table 1).<sup>40</sup> Its 3*R*,5*S* and 3*S*,5*S* stereoisomers, 3 and 4, respectively, were synthesized in an analogous manner beginning with commercially available ethyl (3*S*)-4-chloro-3-hydroxybutanoate. The fully protected intermediates for each of the four epimers were separated by supercritical fluid chromatography, and each was found to be >98% stereopure. Extensive details on synthesis and analysis are provided in the Supporting Information.

**Bacterial Strains.** *E. coli* W3110, MG1655, and BW25113 and single rDNA strain SQ110 were obtained from the Coli Genetic Stock Collection, as were *E. coli* Keio knockout mutant strains containing kanamycin cassette insertions in *dppA* (JW3513), *dppB* (JW3512), *dppC* (JW3511), *dppD* (JW3510), *dppF* (JW3509), *nikA* (JW3441), *oppA* (JW1235), *sapA* (JW1287), *mppA* (JW1322), and *ubiX* (JW2308). *E. coli*  $\Delta dppA$  and *E. coli*  $\Delta ubiX$  were constructed from JW3513 and JW2308, respectively.<sup>41</sup> *E. coli* ATCC25922 was used for mouse models of infection, of which a  $\Delta dppA$  derivative was constructed.<sup>41,42</sup> Construction of the strain was verified by whole genome sequencing, confirming that additional mutations had not been introduced, and the strain was deposited in AstraZeneca's culture collection and is here referred to as *E. coli* ARC5446. Clinical isolates were used to monitor activity against other Gram-negative species: *Pseudomonas aeruginosa* PAO1,<sup>43</sup> *Klebsiella pneumoniae* ARC1865 (obtained as strain EU-050 from G.R. Micro Ltd. (London, UK), and *Acinetobacter baumannii* ARC3495 (obtained as strain 211AN84 from Novexel SA, Romainville, France).

## Coupled in Vitro Transcription–Translation Assays.

Coupled in vitro transcription–translation assays using S30 extract from *E. coli* were performed with modifications in compound preparation.<sup>44</sup> Specifically, compounds were dissolved and serially diluted in water instead of in DMSO. To compensate for the 1% (v/v) DMSO in the reaction, 2% (v/v) DMSO was added to reagent 1, containing S30 extract.

**Susceptibility Determination.** Antimicrobial activity was determined in cation-adjusted Mueller–Hinton broth (MHBII) according to conditions defined by the Clinical and Laboratory Standards Institute,<sup>45</sup> unless M9, with glucose as the carbon source, was used;<sup>46</sup> these are referred to as rich and minimal salts media, respectively. When appropriate, the pH of MHBII was adjusted by the addition of 100 mM K-morpholineethanesulfonic acid for pH 5.5 to 6.5, 100 mM K-N-2-hydroxyethylpiperazine-*N'*-2-ethanesulfonic acid for pH 7 to 8, and 100 mM tris(hydroxymethyl)aminomethane-chloride for a pH above 8.<sup>25</sup>

**Isolation of Negamycin-Resistant Mutants.** Mutants of *E. coli* were isolated as previously described.<sup>47</sup> In short, cell suspensions were prepared by scraping colonies from cultures grown overnight at 37 °C on agar plates containing either M9 + glucose or MHBII medium. Suspensions containing 10<sup>4</sup>–10<sup>9</sup> cells were spread over negamycin-containing plates and incubated for 24–48 h, after which resistant colonies were purified twice on identical plates.

**Whole Genome Sequencing and Analysis.** Genomic DNA purified using the Maxwell 16 cell DNA purification kit (Promega, Madison, WI, USA) and quantified using the Qubit fluorometer (Invitrogen Life Technologies, Grand Island, NY, USA) was used for library construction. DNA libraries were prepared using the Nextera library construction protocol (Illumina, San Diego, CA, USA) following the manufacturer's instructions and sequenced on a MiSeq sequencer (Illumina).



For each isolate, ~2.5 million 150 bp paired-end sequence reads were assembled de novo and analyzed using the CLCBio suite of software tools (Cambridge, MA, USA).

**Assessment of Animal Efficacy.** An animal care and study protocol were used in an Association for Assessment and Accreditation of Laboratory Animal Care International accredited facility, approved by the Institutional Animal Care and Use Committee.

The pharmacokinetics of negamycin stereoisomers in mice was determined following the administration of a single dose of 5 mg/kg as a saline solution (1 mg/mL) to male CD-1 mice (Charles River, Wilmington, MA; mean body weight of 20.8 g,  $n = 9$ ) via the subcutaneous route. Blood samples were collected from the submandibular vein 0.083, 0.25, 0.5, 1, 1.5, 2, 3, 5, and 7 h after dose administration. At each time point, samples from three random mice were taken and three samples per mouse were collected through the course of the experiment. Plasma was obtained by centrifugation at 1000g for 15 min and stored at  $-80\text{ }^{\circ}\text{C}$  until analysis using a recently developed LC-MS/MS method.<sup>16</sup> Plasma PK parameters were calculated using Phoenix WinNonLin software.

The efficacy of negamycin stereoisomers was determined in female CD-1 mice weighing 18–20 g (Charles River) that were rendered neutropenic by intraperitoneal injections of 150 mg/kg cyclophosphamide on day  $-4$  and 100 mg/kg on day  $-1$  prior to infection. Thigh infections were produced by intramuscular injection of the inoculum to target  $10^6$  CFU/thigh.<sup>48</sup> For efficacy studies, compounds were administered in a dose range of 25 to 1000 mg/kg/day in an interval of q4h or q6h by subcutaneous administration, starting 2 h postinfection. Mice were euthanized by  $\text{CO}_2$  exposure just prior to the first administration of the compound (pretreatment group) and 12 and 24 h after treatment initiation (for vehicle control and treatment groups, respectively). Infected thigh muscles were then aseptically removed, weighed, homogenized, and plated on MacConkey agar for the determination of bacterial counts (lower limit of quantification, 100 colony-forming units (CFU)/g). The efficacy of a compound was assessed by the change in thigh burden of the treated groups versus that of the pretreatment group.

**Computational Modeling.** Using the Maestro protocol for flexible alignment,<sup>49</sup> negamycin and its three stereoisomers 3R,5S, 3S,5R, and 3S,5S were aligned with the bound conformation of the Gly-L-Leu dipeptide in such a way as to minimize deviations from the charged groups (C- and N-termini) and the amide bond of Gly-L-Leu. All of the alignments were exhaustively minimized to relax atom clashes that appeared as a result of the difference in size between the compounds and the dipeptide. Then, to extend conformational heterogeneity, Schrödinger's Induced Fit Docking was applied.<sup>50</sup> All docked poses were clustered with a 2 Å clustering radius and rescored by the combined molecular mechanical/generalized Born surface area (MM-GBSA) scoring function.<sup>51</sup>

## ■ ASSOCIATED CONTENT

### 📄 Supporting Information

The following file is available free of charge on the ACS Publications website at DOI: 10.1021/acsinfecdis.5b00027.

Synthesis and analysis of all negamycin stereoisomers in detail. Antimicrobial activity of negamycin and its stereoisomers against a range of Gram-negative pathogens. Genetic changes observed in negamycin-resistant

isolates and pharmacokinetic properties of negamycin stereoisomers upon subcutaneous doing in mice. Synthesis route for negamycin stereoisomers, chemical structures of penultimate, fully protected stereoisomer precursors, chromatograms validating their respective chiral centers, and time courses of the establishment of infections by *E. coli* ATCC25992 and ARC5446 in the thighs of neutropenic mice (PDF).

## ■ AUTHOR INFORMATION

### Corresponding Author

\*E-mail: Ed.Buurman@astrazeneca.com.

### Present Addresses

(N.B.-S.): Oncology Innovative Medicines Unit, AstraZeneca R&D Boston, Waltham, Massachusetts 02451, United States.

(J.G.): Celgene Avilomics Research, 45 Wiggins Avenue, Bedford, Massachusetts 01730, United States.

(A.M.R.): Schrödinger, Inc., 245 First Street, Cambridge, Massachusetts 02142, United States.

### Notes

The authors declare the following competing financial interest(s): All authors were AstraZeneca employees at the time this work was performed and may as a result own company stock.

## ■ ACKNOWLEDGMENTS

Negamycin was synthesized chemically in collaboration with the Pharmaron Corporation.

## ■ REFERENCES

- (1) Ames, B. N., Ames, G. F., Young, J. D., Tsuchiya, D., and Lecocq, J. (1973) Illicit transport: the oligopeptide permease. *Proc. Natl. Acad. Sci. U. S. A.* 70, 456–458.
- (2) Ames, G. F., and Roth, J. R. (1968) Histidine and aromatic permeases of *Salmonella typhimurium*. *J. Bacteriol.* 96, 1742–1749.
- (3) Luckey, M., Pollack, J. R., Wayne, R., Ames, B. N., and Neilands, J. B. (1972) Iron uptake in *Salmonella typhimurium*: utilization of exogenous siderochromes as iron carriers. *J. Bacteriol.* 111, 731–738.
- (4) Stefanska, A. L., Fulston, M., Houge-Frydrych, C. S., Jones, J. J., and Warr, S. R. (2000) A potent seryl tRNA synthetase inhibitor SB-217452 isolated from a *Streptomyces* species. *J. Antibiot.* 53, 1346–1353.
- (5) Kahan, F. M., Kahan, J. S., Cassidy, P. J., and Kropp, H. (1974) The mechanism of action of fosfomycin (phosphonomycin). *Ann. N. Y. Acad. Sci.* 235, 364–386.
- (6) Kanimoto, Y., and Greenwood, D. (1987) Comparison of the response of *Escherichia coli* to fosfomycin and fosmidomycin. *Eur. J. Clin. Microbiol.* 6, 386–391.
- (7) Kojo, H., Shigi, Y., and Nishida, M. (1980) FR-31564, a new phosphonic acid antibiotic: bacterial resistance and membrane permeability. *J. Antibiot.* 33, 44–48.
- (8) Kuzuyama, T., Shimizu, T., Takahashi, S., and Seto, H. (1998) Fosmidomycin, a specific inhibitor of 1-deoxy-D-xylulose 5-phosphate reductoisomerase in the nonmevalonate pathway for terpenoid biosynthesis. *Tetrahedron Lett.* 39, 7913–7916.
- (9) Kondo, S., Shibahara, S., Takahashi, S., Maeda, K., and Umezawa, H. (1971) Negamycin, a novel hydrazide antibiotic. *J. Am. Chem. Soc.* 93, 6305–6306.
- (10) Hamada, M., Takeuchi, T., Kondo, S., Ikeda, Y., and Naganawa, H. (1970) A new antibiotic, negamycin. *J. Antibiot.* 23, 170–171.
- (11) Uehara, Y., Kondo, S., Umezawa, H., Suzukake, K., and Hori, M. (1972) Negamycin, a miscoding antibiotic with a unique structure. *J. Antibiot.* 25, 685–688.

- (12) Rice, L. B. (2008) Federal funding for the study of antimicrobial resistance in nosocomial pathogens: no ESKAPE. *J. Infect. Dis.* 197, 1079–1081.
- (13) Olivier, N. B., Altman, R. B., Noeske, J., Basarab, G. S., Code, E., Ferguson, A. D., Gao, N., Huang, J., Juetter, M. F., Livchak, S., Miller, M. D., Prince, D. B., Cate, J. H., Buurman, E. T., and Blanchard, S. C. (2014) Negamycin induces translational stalling and miscoding by binding to the small subunit head domain of the *Escherichia coli* ribosome. *Proc. Natl. Acad. Sci. U. S. A.* 111, 16274–16279.
- (14) Polikanov, Y. S., Szal, T., Jiang, F., Gupta, P., Matsuda, R., Shiozuka, M., Steitz, T. A., Vázquez-Laslop, N., and Mankin, A. S. (2014) Negamycin interferes with decoding and translocation by simultaneous interaction with rRNA and tRNA. *Mol. Cell* 56, 541–550.
- (15) Jenner, L., Starosta, A. L., Terry, D. S., Mikolajka, A., Filonava, L., Yusupov, M., Blanchard, S. C., Wilson, D. N., and Yusupova, G. (2013) Structural basis for potent inhibitory activity of the antibiotic tigecycline during protein synthesis. *Proc. Natl. Acad. Sci. U. S. A.* 110, 3812–3816.
- (16) Guo, J., Miele, E. M., Chen, A., Luzietti, R. A., Zambrowski, M., Walsky, R. L., Buurman, E. T. (2015) Pharmacokinetics of the natural antibiotic negamycin. *Xenobiotica* 45, in press.10.3109/00498254.2015.1006301
- (17) Raju, B., Mortell, K., Anandan, S., O'Dowd, H., Gao, H., Gomez, M., Hackbarth, C., Wu, C., Wang, W., Yuan, Z., White, R., Trias, J., and Patel, D. V. (2003) N- and C-terminal modifications of negamycin. *Bioorg. Med. Chem. Lett.* 13, 2413–2418.
- (18) Abouhamad, W. N., and Manson, M. D. (1994) The dipeptide permease of *Escherichia coli* closely resembles other bacterial transport systems and shows growth-phase-dependent expression. *Mol. Microbiol.* 14, 1077–1092.
- (19) Mahoney, T. F., and Silhavy, T. J. (2013) The Cpx stress response confers resistance to some, but not all, bactericidal antibiotics. *J. Bacteriol.* 195, 1869–1874.
- (20) Stabb, E. V., and Handelsman, J. (1998) Genetic analysis of zwittermixin A resistance in *Escherichia coli*: effects on membrane potential and RNA polymerase. *Mol. Microbiol.* 27, 311–322.
- (21) Baisa, G., Stabo, N. J., and Welch, R. A. (2013) Characterization of *Escherichia coli* D-cycloserine transport and resistant mutants. *J. Bacteriol.* 195, 1389–1399.
- (22) Higgins, C. F., and Ames, G. F. (1981) Two periplasmic transport proteins which interact with a common membrane receptor show extensive homology: complete nucleotide sequences. *Proc. Natl. Acad. Sci. U. S. A.* 78, 6038–6042.
- (23) Manson, M. D., Blank, V., Brade, G., and Higgins, C. F. (1986) Peptide chemotaxis in *E. coli* involves the Tap signal transducer and the dipeptide permease. *Nature* 321, 253–256.
- (24) Smith, M. W., Tyreman, D. R., Payne, G. M., Marshall, N. J., and Payne, J. W. (1999) Substrate specificity of the periplasmic dipeptide-binding protein from *Escherichia coli*: experimental basis for the design of peptide prodrugs. *Microbiology* 145, 2891–2901.
- (25) Damper, P. D., and Epstein, W. (1981) Role of the membrane potential in bacterial resistance to aminoglycoside antibiotics. *Antimicrob. Agents Chemother.* 20, 803–808.
- (26) Nikaido, H., and Thanassi, D. G. (1993) Penetration of lipophilic agents with multiple protonation sites into bacterial cells: tetracyclines and fluoroquinolones as examples. *Antimicrob. Agents Chemother.* 37, 1393–1399.
- (27) Rigler, N. E., Bag, S. P., Leyden, D. E., Sudmeier, J. L., and Reilley, C. N. (1965) Determination of a protonation scheme of tetracycline using nuclear magnetic resonance. *Anal. Chem.* 37, 872–875.
- (28) Dunten, P., and Mowbray, S. L. (1995) Crystal structure of the dipeptide binding protein from *Escherichia coli* involved in active transport and chemotaxis. *Protein Sci.* 4, 2327–2334.
- (29) Nickitenko, A. V., Trakhanov, S., and Quiocho, F. A. (1995) 2 Å resolution structure of DppA, a periplasmic dipeptide transport/chemosensory receptor. *Biochemistry* 34, 16585–16595.
- (30) Payne, J. W., Grail, B. M., Gupta, S., Ladbury, J. E., Marshall, N. J., O'Brien, R., and Payne, G. M. (2000) Structural basis for recognition of dipeptides by peptide transporters. *Arch. Biochem. Biophys.* 384, 9–23.
- (31) Li, C. Y., Chen, X. L., Qin, Q. L., Wang, P., Zhang, W. X., Xie, B. B., Su, H. N., Zhang, X. Y., Zhou, B. C., and Zhang, Y. Z. (2015) Structural insights into the multispecific recognition of dipeptides of deep-sea Gram-negative bacterium *Pseudoalteromonas sp.* SM9913. *J. Bacteriol.* 197, 1125–1134.
- (32) Benz, R., Janko, K., and Lauger, P. (1979) Ionic selectivity of pores formed by the matrix protein (porin) of *Escherichia coli*. *Biochim. Biophys. Acta, Biomembr.* 551, 238–247.
- (33) Nikaido, H., and Rosenberg, E. Y. (1983) Porin channels in *Escherichia coli*: studies with liposomes reconstituted from purified proteins. *J. Bacteriol.* 153, 241–252.
- (34) Li, Z., Nimitz, M., and Rinas, U. (2014) The metabolic potential of *Escherichia coli* BL21 in defined and rich medium. *Microb. Cell Fact.* 13, 45.
- (35) Padan, E., Zilberstein, D., and Rottenberg, H. (1976) The proton electrochemical gradient in *Escherichia coli* cells. *Eur. J. Biochem.* 63, 533–541.
- (36) Bryan, L. E., and Van Den Elzen, H. M. (1977) Effects of membrane-energy mutations and cations on streptomycin and gentamicin accumulation by bacteria: a model for entry of streptomycin and gentamicin in susceptible and resistant bacteria. *Antimicrob. Agents Chemother.* 12, 163–177.
- (37) Tomaras, A. P., Crandon, J. L., McPherson, C. J., Banevicius, M. A., Finegan, S. M., Irvine, R. L., Brown, M. F., O'Donnell, J. P., and Nicolau, D. P. (2013) Adaptation-based resistance to siderophore-conjugated antibacterial agents by *Pseudomonas aeruginosa*. *Antimicrob. Agents Chemother.* 57, 4197–4207.
- (38) Zhanel, G. G., Lawson, C. D., Zelenitsky, S., Findlay, B., Schweizer, F., Adam, H., Walkty, A., Rubinstein, E., Gin, A. S., Hoban, D. J., Lynch, J. P., and Karlowsky, J. A. (2012) Comparison of the next-generation aminoglycoside plazomicin to gentamicin, tobramycin and amikacin. *Expert Rev. Anti-Infect. Ther.* 10, 459–473.
- (39) Thulin, E., Sundqvist, M., and Andersson, D. I. (2015) Amdinocillin (mecillinam) resistance mutations in clinical isolates and laboratory-selected mutants of *Escherichia coli*. *Antimicrob. Agents Chemother.* 59, 1718–1727.
- (40) Davies, S. G., Ichihara, O., Roberts, P. M., and Thomson, J. E. (2011) Asymmetric syntheses of (+)-negamycin, (+)-3-epi-negamycin and sperabillin C via lithium amide conjugate addition. *Tetrahedron* 67, 216–227.
- (41) Datsenko, K. A., and Wanner, B. L. (2000) One-step inactivation of chromosomal genes in *Escherichia coli* K-12 using PCR products. *Proc. Natl. Acad. Sci. U. S. A.* 97, 6640–6645.
- (42) Baba, T.; Ara, T.; Hasegawa, M.; Takai, Y.; Okumura, Y.; Baba, M.; Datsenko, K. A.; Tomita, M.; Wanner, B. L.; Mori, H. Construction of *Escherichia coli* K-12 in-frame, single-gene knockout mutants: the Keio collection. *Mol. Syst. Biol.* 2006, 2, DOI: 10.1038/msb4100050.
- (43) Masuda, N., Sakagawa, E., Ohya, S., Gotoh, N., Tsujimoto, H., and Nishino, T. (2000) Substrate specificities of MexAB-OprM, MexCD-OprJ, and MexXY-oprM efflux pumps in *Pseudomonas aeruginosa*. *Antimicrob. Agents Chemother.* 44, 3322–3327.
- (44) Buurman, E. T., Foulk, M. A., Gao, N., Laganas, V. A., McKinney, D. C., Moustakas, D. T., Rose, J. A., Shapiro, A. B., and Fleming, P. R. (2012) Novel rapidly diversifiable antimicrobial RNA polymerase switch region inhibitors with confirmed mode of action in *Haemophilus influenzae*. *J. Bacteriol.* 194, 5504–5512.
- (45) Clinical and Laboratory Standards Institute *Methods for Dilution Antimicrobial Susceptibility Tests for Bacteria That Grow Aerobically*, 9th ed.; Approved Standard M07-A8; Clinical and Laboratory Standards Institute: Wayne, PA, 2009; Vol. 29, no. 2.
- (46) Sambrook, J.; Russell, D. W. *Molecular Cloning: A Laboratory Manual*, 2nd ed.; Cold Spring Harbor, New York, 2001.
- (47) Buurman, E. T., Johnson, K. D., Kelly, R. K., and MacCormack, K. (2006) Different modes of action of naphthyridones in Gram-



positive and Gram-negative bacteria. *Antimicrob. Agents Chemother.* 50, 385–387.

(48) Craig, W. A. (1998) Pharmacokinetic/pharmacodynamic parameters: rationale for antibacterial dosing of mice and men. *Clin. Infect. Dis.* 26, 1–10.

(49) Schrödinger; *Schrödinger*, Release 2014–3: Maestro, version 9.9.; Schrödinger, LLC: New York, 2014.

(50) Sherman, W., Day, T., Jacobson, M. P., Friesner, R. A., and Farid, R. (2006) Novel procedure for modeling ligand/receptor induced fit effects. *J. Med. Chem.* 49, 534–553.

(51) Sirin, S., Kumar, R., Martinez, C., Karmilowicz, M. J., Ghosh, P., Abramov, Y. A., Martin, V., and Sherman, W. (2014) A computational approach to enzyme design: predicting omega-aminotransferase catalytic activity using docking and MM-GBSA scoring. *J. Chem. Inf. Model.* 54, 2334–2346.

(52) Schrödinger; *The PyMOL Molecular Graphics System*, Version 1.7.4; Schrödinger, LLC: New York, 2014.